atoms

MDPI

Article

A Complete CDW Theory for the Single Ionization of Multielectronic Atoms by Bare Ion Impact

Juan M. Monti *, Michele A. Quinto and Roberto D. Rivarola

Laboratorio de Colisiones Atómicas, Facultad de Ciencias Exactas, Ingeniería y Agrimensura, and Instituto de Física Rosario (CONICET-UNR), Universidad Nacional de Rosario, Avenida Pellegrini 250, Rosario 2000, Argentina; quinto@ifir-conicet.gov.ar (M.A.Q.); rivarola@ifir-conicet.gov.ar (R.D.R.)

* Correspondence: monti@ifir-conicet.gov.ar

Abstract: A complete form of the post version of the continuum distorted wave (CDW) theory is used to investigate the single ionization of multielectronic atoms by fast bare heavy ion beams. The influence of the non-ionized electrons on the dynamic evolution is included through a residual target potential considered as a non-Coulomb central potential through a GSZ parametric one. Divergences found in the transition amplitude containing the short-range part of the target potential are avoided by considering, in that term exclusively, an eikonal phase instead of the continuum factor as the initial channel distortion function. In this way, we achieve the inclusion of the interaction between the target active electron and the residual target, giving place to a more complete theory. The present analysis is supported by comparisons with existing experimental electron emission spectra and other distorted wave theories.

Keywords: ionization; distorted wave theories; multielectronic atoms; heavy ions

Citation: Monti, J.M.; Quinto, M.A.; Rivarola, R.D. A Complete CDW Theory for the Single Ionization of Multielectronic Atoms by Bare Ion Impact. *Atoms* **2021**, *9*, 3. https://doi.org/10.3390/atoms9010003

Received: 1 December 2020
Accepted: 6 January 2021
Published: 13 January 2021

1. Introduction

The present work deals with the single ionization of atoms by fast bare ion impact within the continuum distorted wave (CDW) [1] and the continuum distorted wave-eikonal initial state (CDW-EIS) [2] distorted wave theories. Originally, the three-body CDW and CDW-EIS distorted wave theories were developed to investigate ion-atom processes for monoelectronic targets. They were introduced in order to accelerate the convergence of a Born series description. Later, an extension of the CDW-EIS description for the single ionization of multielectronic targets was made by Fainstein et al. [3]. They reduced the multielectronic case to a monoelectronic treatment within a three-body approximation, the three bodies considered being the projectile, the residual target, and the active electron (the one to be ionized as a consequence of the collision). The other electrons, the passive ones, were supposed to remain as frozen in their initial orbitals during the reaction (see [3]). This allowed the extension of these distorted theories to complex electronic systems. Since that time, they were used in a reliable way to calculate the differential, as well as the total cross-section for a wide variety of collision systems with projectiles ranging from antiprotons to highly-charged bare ions and targets going from atoms to a large diversity of molecules [3–9]. In the distorted wave formalism, the action of the perturbative potentials can either be applied to the initial channel distorted wave function or to the final channel distorted one, giving place to the prior and post versions of the transition matrix element, respectively [10,11]. To calculate them, effective Coulomb potentials were chosen to represent the interaction between the residual target and the active electron (the ionized one) in the exit channel. The use of this Coulombic potential gave place to post-prior discrepancies [12,13]. In a previous work [14], we revisited the formulation of the post version of the CDW-EIS approximation, showing that the inclusion of an additional potential in the exit channel, which was neglected in the previous post version calculations, almost completely removes these discrepancies. This potential is associated with a first-order description of

the dynamic screening produced by the passive electrons on the evolution of the active one. In this work, we deal with the post-prior discrepancies in the CDW theory and the inclusion of the dynamic screening in the post-CDW theory. It has been shown (see [15]) that the prior version of the CDW theory for single ionization has an intrinsic logarithmic divergence near the binary-encounter peak, which prevents the transition amplitude from being integrated in order to obtain the differential and total cross-sections. Although there was an abstract sent by Dubé and Dewangan to the ICPEACXIX Conference [16] stating that an integration of such divergences was feasible, to the best of our knowledge, there is no further evidence or proof of how to perform such an integration. In this paper, we study the terms containing the logarithmic divergences present in both the post and prior versions of the CDW theory, and we propose a way of including the dynamic screening in the post-CDW theory without encountering such divergences. Atomic units will be used throughout this work unless otherwise stated.

2. Theory

The CDW theory was initially developed to study single electron capture, and later single electron ionization, from monoelectronic targets by bare projectile impact [1,17,18]. The extension to multielectronic targets can be made following the work by Fainstein et al. [3] (see also [4,19] and the references therein), where it was shown that, for single ionization from bare ion impact, within the independent electron model, a multielectronic system can be reduced to a monoelectronic one. Within the independent electron model, and considering one active electron (the one to be ionized), the target potential V_T can be written as:

$$V_T(\boldsymbol{x}) = -\frac{Z_T}{x} + V_{ap}(\boldsymbol{x}), \tag{1}$$

where $\boldsymbol{x}$ is the active electron coordinate in the target reference frame. The first term describes the Coulomb interaction between the active-electron and the target nuclear charge Z_T, whereas the second one involves the electrostatic interaction between the active electron and the passive ones (see [14]).

The CDW approximation is the first-order of a distorted wave series in which the initial and final distorted waves are proposed as:

$$\begin{aligned} \chi_i^+(\boldsymbol{x},t) &= \Phi_i(\boldsymbol{x},t)\,\mathcal{L}_i^+(\boldsymbol{s}) && (2)\\ &= \phi_i(\boldsymbol{x})\exp\left(-\mathrm{i}\,\varepsilon_i t\right)\mathcal{L}_i^+(\boldsymbol{s}) && (3)\\ \chi_f^-(\boldsymbol{x},t) &= \Phi_f(\boldsymbol{x},t)\,\mathcal{L}_f^-(\boldsymbol{s}) && (4)\\ &= \phi_f(\boldsymbol{x})\exp\left(-\mathrm{i}\,\varepsilon_f t\right)\mathcal{L}_f^-(\boldsymbol{s}), && (5) \end{aligned}$$

respectively. In (2) and (4), $\Phi_i(\boldsymbol{x},t)$ and $\Phi_f(\boldsymbol{x},t)$ are the initial-bound and final-continuum state solutions of the time-dependent target Schrödinger equation. In (3), ε_i is the electron energy in the initial bound state, whereas in (5), $\varepsilon_f = \frac{1}{2}k^2$ is the electron energy in the final state, $\boldsymbol{k}$ being the linear momentum of the ejected electron in the target reference frame.

The initial distortion is proposed as:

$$\mathcal{L}_i^+(\boldsymbol{s}) = N(\nu)\,{}_1F_1[\mathrm{i}\nu;1;\mathrm{i}\,(vs+\boldsymbol{v}\cdot\boldsymbol{s})], \tag{6}$$

whereas the final distortion is chosen as:

$$\mathcal{L}_f^-(\boldsymbol{s}) = N^*(\zeta)\,{}_1F_1[-\mathrm{i}\zeta;1;-\mathrm{i}\,(ps+\boldsymbol{p}\cdot\boldsymbol{s})] \tag{7}$$

where $\boldsymbol{v}$ is the projectile velocity, $\nu = Z_P/v$, $\zeta = Z_P/p$, $\boldsymbol{p} = \boldsymbol{k} - \boldsymbol{v}$ the ejected electron momentum in the projectile reference frame, and $N(a) = \exp(\pi a/2)\Gamma(1+ia)$ (with Γ being Euler's Gamma function) is the normalization factor of the ${}_1F_1$ hypergeometric function.

The initial-bound state of the target ϕ_i and its binding energy ε_i in (3) are calculated by means of RHFwavefunctions (see [20] and the Appendix in [11]). On the other hand,

the target final continuum state ϕ_f is chosen as an analytical hydrogen-like continuum function:

$$\phi_f(\boldsymbol{x}) = \frac{1}{(2\pi)^{3/2}} \exp(\mathrm{i}\,\boldsymbol{k}\cdot\boldsymbol{x}) \times N^*(\lambda)\,{}_1F_1[-\mathrm{i}\,\lambda, 1, -\mathrm{i}\,(kx + \boldsymbol{k}\cdot\boldsymbol{x})], \tag{8}$$

$\lambda = \tilde{Z}_T/k$ with $\tilde{Z}_T$ being an effective or net target charge to be chosen.

Finally, the double differential cross-section in electron emission energy (E_k) and solid ejection angles is obtained as (see [14]):

$$\frac{d^2\sigma^{\pm}}{dE_k d\Omega_k} = k \int d\boldsymbol{\eta} \left|\mathcal{R}^{\pm}_{if}(\boldsymbol{\eta})\right|^2 \tag{9}$$

$\mathcal{R}^{\pm}_{if}(\boldsymbol{\eta})$ being the scattering matrix element as a function of the transverse momentum transfer $\boldsymbol{\eta}$, with the $-$ $(+)$ sign denoting its prior (post) form.

2.1. Prior Version of the CDW Approximation

W^+ is the prior CDW perturbative operator defined by:

$$W^+\,\chi_i^+ = \Phi_i(\boldsymbol{x}, t)\left[\boldsymbol{\nabla}_{\boldsymbol{x}} \ln\phi_i(\boldsymbol{x}) \cdot \boldsymbol{\nabla}_{\boldsymbol{s}} \mathcal{L}_i^+(\boldsymbol{s})\right]. \tag{10}$$

Using the well-known Fourier transform method, the transition amplitude for the prior version of the CDW results:

$$\mathcal{R}^-_{if}(\boldsymbol{\eta}) = -\mathrm{i}\frac{4\pi^2}{v}\boldsymbol{F}^-(\boldsymbol{K})\cdot\boldsymbol{G}^-(\boldsymbol{K}) \tag{11}$$

being:

$$\boldsymbol{K} = -\boldsymbol{\eta} - \frac{\Delta\varepsilon}{v}\hat{\boldsymbol{v}} \tag{12}$$

with $\Delta\varepsilon = \varepsilon_f - \varepsilon_i$ and:

$$\boldsymbol{F}^-(\boldsymbol{K}) = \frac{-1}{(2\pi)^{3/2}} \int d\boldsymbol{x}\, \exp\left(-\mathrm{i}\boldsymbol{K}\cdot\boldsymbol{x}\right)\phi_f^*(\boldsymbol{x})\boldsymbol{\nabla}_{\boldsymbol{x}}\,\phi_i(\boldsymbol{x}) \tag{13}$$

$$\boldsymbol{G}^-(\boldsymbol{K}) = \frac{1}{(2\pi)^{3/2}} \int d\boldsymbol{s}\, \exp\left(\mathrm{i}\boldsymbol{K}\cdot\boldsymbol{s}\right)\mathcal{L}_f^{-*}(\boldsymbol{s})\boldsymbol{\nabla}_{\boldsymbol{s}}\,\mathcal{L}_i^+(\boldsymbol{s}). \tag{14}$$

The $\boldsymbol{F}^-$ factor is the same as in the prior version of the CDW-EIS theory for ionization when working with initial target bound states described as a linear combination of Slater-type functions (see Appendix A and [11]); whereas, the $\boldsymbol{G}^-$ factor is a Nordsieck integral (see [21]) given by:

$$\boldsymbol{G}^-(\boldsymbol{K}) = \frac{\mathrm{i}\nu}{(2\pi)^{1/2}} \frac{N(\nu)N(\xi)}{\alpha(\alpha+\beta)} \left(\frac{\gamma+\delta}{\gamma}\right)^{-\mathrm{i}\nu} \left(\frac{\gamma}{\alpha}\right)^{-\mathrm{i}\xi} \times \left\{ \mathrm{i}v\xi \left[\frac{(\alpha+\beta)}{(\gamma+\delta)}(p\hat{\boldsymbol{v}} - \boldsymbol{p} - \boldsymbol{K}) + \boldsymbol{K}\right] {}_2F_1[1+\mathrm{i}\nu, 1-\mathrm{i}\xi, 2, z] - v\boldsymbol{K}\,{}_2F_1[\mathrm{i}\nu, 1-\mathrm{i}\xi, 1, z] \right\} \tag{15}$$

with:

$$z = \frac{\alpha\delta - \beta\gamma}{\alpha(\gamma+\delta)} \tag{16}$$

being:

$$\alpha = \frac{1}{2}K^2 \tag{17}$$

$$\beta = -\Delta\varepsilon \tag{18}$$

$$\delta = \beta + \boldsymbol{p}\cdot\boldsymbol{v} - p\,v \tag{19}$$

$$\gamma = \alpha + \boldsymbol{p}\cdot\boldsymbol{K}. \tag{20}$$

2.2. Post Version of the CDW Approximation

With the above choice given in (8) for ϕ_f, the function Φ_f in (5) is, therefore, the solution of the Schrödinger equation:

$$\left(-\frac{1}{2}\nabla_x^2 - \frac{\tilde{Z}_T}{x} - \mathrm{i}\frac{\partial}{\partial t}\bigg|_x\right)\Phi_f(\boldsymbol{x},t) = 0. \tag{21}$$

W^- is given by:

$$W_f^-\chi_f^- = \Phi_f(\boldsymbol{x},t)\left[\boldsymbol{\nabla}_{\boldsymbol{x}}\ln\phi_f(\boldsymbol{x})\cdot\boldsymbol{\nabla}_{\boldsymbol{s}}\mathcal{L}_f^-(\boldsymbol{s})\right] + \tilde{V}_T(\boldsymbol{x})\chi_f^-, \tag{22}$$

where the first term is the well-known post CDW perturbative operator and the second one is related to an additional potential left unsolved by the choice of ϕ_f:

$$\tilde{V}_T(\boldsymbol{x}) = -(Z_T - \tilde{Z}_T)/x + V_{ap}(\boldsymbol{x}), \tag{23}$$

$V_{ap}(\boldsymbol{x})$ being the interaction between the active electron and the passive ones [14]. This $\tilde{V}_T$ potential is excluded in the usual post version of the CDW theory. We choose $\tilde{Z}_T = n_i\sqrt{-2\varepsilon_i}$ (see [18]), with n_i the principal quantum number of the initial bound orbital, as the effective charge describing the hydrogen-like continuum for the residual target continuum final state.

Following the work of [11], we consider $\tilde{V}_T$ in terms of a GSZ analytical parametric potential [22], and re-write (23), resulting in:

$$\tilde{V}_T(\boldsymbol{x}) = -\frac{(q-\tilde{Z}_T)}{x} - \frac{(Z_T-q)}{x}\Omega(x) \tag{24}$$

with:

$$\Omega(x) = \left[H\left(e^{x/d}-1\right)+1\right]^{-1}, \tag{25}$$

$q = Z_T - N$ being the net charge of the target, with N the number of passive electrons, and H and d parameters depending on Z_T and N (see [22] and the references therein). The parameters used for each target are shown in Table 1.

Table 1. Parameters d and K of the GSZ potential for the different targets considered, extracted from [22].

Target	d (a.u.)	K (a.u.)
He	0.381	1.77
Ne	0.558	2.71
Ar	1.045	3.50

Proceeding as in the case of the prior version, the transition amplitude for the post version of the CDW results in:

$$\mathcal{R}_{if}^+(\boldsymbol{\eta}) = -\mathrm{i}\frac{4\pi^2}{v}\left[\boldsymbol{F}^{a+}(\boldsymbol{K})\cdot\boldsymbol{G}^{a+}(\boldsymbol{K}) + F^{b+}(\boldsymbol{K})G^{b+}(\boldsymbol{K})\right] \tag{26}$$

$$\boldsymbol{F}^{a+}(\boldsymbol{K}) = \frac{-1}{(2\pi)^{3/2}} \int d\boldsymbol{x}\, \exp\left(-\mathrm{i}\boldsymbol{K}\cdot\boldsymbol{x}\right)\phi_i(\boldsymbol{x})\boldsymbol{\nabla}_{\boldsymbol{x}}\,\phi_f^*(\boldsymbol{x}) \tag{27}$$

$$\boldsymbol{G}^{a+}(\boldsymbol{K}) = \frac{1}{(2\pi)^{3/2}} \int d\boldsymbol{s}\, \exp\left(\mathrm{i}\boldsymbol{K}\cdot\boldsymbol{s}\right)\mathcal{L}_i^+(\boldsymbol{s})\boldsymbol{\nabla}_{\boldsymbol{s}}\,\mathcal{L}_f^{-*}(\boldsymbol{s}) \tag{28}$$

$$F^{b+}(\boldsymbol{K}) = \frac{1}{(2\pi)^{3/2}} \int d\boldsymbol{x}\, \exp\left(-\mathrm{i}\boldsymbol{K}\cdot\boldsymbol{x}\right)\tilde{V}_T(\boldsymbol{x})\phi_i(\boldsymbol{x})\,\phi_f^*(\boldsymbol{x}) \tag{29}$$

$$G^{b+}(\boldsymbol{K}) = \frac{1}{(2\pi)^{3/2}} \int d\boldsymbol{s}\, \exp\left(\mathrm{i}\boldsymbol{K}\cdot\boldsymbol{s}\right)\mathcal{L}_i^+(\boldsymbol{s})\,\mathcal{L}_f^{-*}(\boldsymbol{s}). \tag{30}$$

When considering only the first term of Equation (26), one gets the usual post version of the CDW, whereas when both terms are considered, the complete post version of the CDW is obtained. The influence of the second term of Equation (26), which contains a residual part of the target dynamic screening, was investigated for the case of the CDW-EIS theory by Monti et al. ([11,14]).

The $\boldsymbol{F}^{a+}$ and F^{b+} factors are the same as in the post version of the CDW-EIS theory for ionization when working with initial target bound states described as a linear combination of Slater-type functions (see Appendix A and [11]); whereas, the $\boldsymbol{G}^{a+}$ and G^{b+} factors are Nordsieck integrals ([21]) given by:

$$\begin{aligned}\boldsymbol{G}^{a+}(\boldsymbol{K}) =& \frac{\mathrm{i}\xi}{(2\pi)^{1/2}}\frac{N(\nu)N(\xi)}{\alpha\gamma}\left(\frac{\gamma}{\alpha}\right)^{-\mathrm{i}\xi}\left(\frac{\gamma+\delta}{\gamma}\right)^{-\mathrm{i}\nu}\\ &\times\left[\mathrm{i}\,p\nu\frac{\gamma}{\gamma+\delta}\left(v\hat{\boldsymbol{p}}-\boldsymbol{v}+\frac{\delta}{\gamma}\boldsymbol{K}\right){}_2F_1[1+\mathrm{i}\nu,1-\mathrm{i}\xi,2,z]-p\boldsymbol{K}\,{}_2F_1[\mathrm{i}\nu,1-\mathrm{i}\xi,1,z]\right]\end{aligned} \tag{31}$$

$$\begin{aligned}G^{b+}(\boldsymbol{K}) =& \frac{1}{(2\pi)^{1/2}}\frac{N(\nu)N(\xi)}{\alpha}\left(\frac{\gamma}{\alpha}\right)^{-\mathrm{i}\xi}\left(\frac{\gamma+\delta}{\gamma}\right)^{-\mathrm{i}\nu}\\ &\times\left[\left(\frac{\xi\,p}{\gamma}+\frac{\nu\,v}{\alpha+\beta}\right){}_2F_1[\mathrm{i}\nu,1-\mathrm{i}\xi,1,z]+\right.\\ &\left.+(-\mathrm{i})\frac{\xi\nu}{\gamma+\delta}\left(p\frac{\delta}{\gamma}+v\frac{(\gamma+\delta-\alpha-\beta)}{\alpha+\beta}\right){}_2F_1[1+\mathrm{i}\nu,1-\mathrm{i}\xi,2,z]\right]\end{aligned} \tag{32}$$

with z, α, β, δ, and γ as defined in Equations (16)–(20).

2.3. Complete Hybrid Post CDW

The divergences arising from the presence of the $1/(\alpha+\beta)$ factor are only avoided when working with the usual post version of the CDW (Equations (27) and (28)) as the term G^{b+} (Equation 32) is neglected. Therefore, in order to include the dynamic screening in the CDW theory, one should consider the complete post or the prior versions, and then, the divergences appearing when $\alpha+\beta=0$ are unavoidable. A possible solution is to approximate, in Equation (30), the asymptotic expression of the initial channel distortion factor $\mathcal{L}_i^+$ (defined in Equation (6)), i.e., an eikonal phase, as in the CDW-EIS theory, defined by:

$$\lim_{vs\to\infty}\mathcal{L}_i^+(\boldsymbol{s}) \equiv \mathcal{L}_i^{EIS,+}(\boldsymbol{s}) = \exp\left[-\mathrm{i}\nu\ln\left(vs+\boldsymbol{v}\cdot\boldsymbol{s}\right)\right]. \tag{33}$$

With this approximation, Equation (30) results in:

$$\begin{aligned}G^{EIS,b+}(\boldsymbol{K}) =& \frac{p\xi}{(2\pi)^{1/2}}\frac{N(\nu)N(\xi)}{\alpha}\left(\frac{\gamma}{\alpha}\right)^{-\mathrm{i}\xi}\left(\frac{\beta}{\alpha}\right)^{-\mathrm{i}\nu}\\ &\times\left[\left(\frac{1}{\gamma}+\frac{1}{\beta}\right){}_2F_1[\mathrm{i}\nu,\mathrm{i}\xi,1,z']+\right.\\ &\left.+(-\mathrm{i})\frac{\alpha}{\beta\gamma}\left(\nu\frac{\delta}{\gamma}+\xi\frac{(\delta-\beta)}{\beta}\right){}_2F_1[1+\mathrm{i}\nu,1+\mathrm{i}\xi,2,z']\right]\end{aligned} \tag{34}$$

with z' defined by:

$$z' = \frac{\beta\gamma - \alpha\delta}{\beta\gamma}. \tag{35}$$

The transition amplitude in this theory results in:

$$\mathcal{R}^{+}_{if}(\boldsymbol{\eta}) = -\mathrm{i}\frac{4\pi^2}{v}\left[\boldsymbol{F}^{a+}(\boldsymbol{K})\cdot\boldsymbol{G}^{a+}(\boldsymbol{K}) + F^{b+}(\boldsymbol{K})G^{EIS,b+}(\boldsymbol{K})\right] \tag{36}$$

This transition amplitude does not contain any term with the $1/(\alpha+\beta)$ factor and also takes into account the dynamic screening as in the CDW-EIS theory.

2.4. Study of the Divergences in the CDW Theory

The integration of the transition amplitude over the transverse momentum transfer $\boldsymbol{\eta}$ can be also performed integrating over the total momentum transfer $\boldsymbol{K}$, given $\boldsymbol{K} = -\boldsymbol{\eta} - \Delta\varepsilon/v$. Then, the DDCSresults:

$$\frac{d^2\sigma^{\pm}}{dE_k d\Omega_k} = k\int d\boldsymbol{K}\left|\mathcal{R}^{\pm}_{if}(\boldsymbol{K})\right|^2 = k\int_0^{2\pi} d\theta_K \int_{K_{min}}^{+\infty} dK\left|\mathcal{R}^{\pm}_{if}(\boldsymbol{K})\right|^2, \tag{37}$$

with $K_{min} = \Delta\varepsilon/v$. It can be seen than $\alpha+\beta = 0$ for a particular value of the momentum transfer given by $K' = \sqrt{2\Delta\varepsilon}$. Furthermore, the lower limit of the integral over K will coincide with K' when the momentum of the emitted electron is $k' = \sqrt{4v^2 + 2\varepsilon_i}$. As k' depends on the projectile velocity and also the binding energy of the initial state, it will have a different value for different shells. Moreover, k' will have a real value for impact velocities $v > -\varepsilon_i/2$. For k-momentum values lower than k', the K' value always falls into the integration interval, whilst for k values larger than k', K_{min} results in being larger than K', and thus, $\alpha+\beta \neq 0$ over all the integration interval. Therefore, in those cases where either no real values of k' exist or when the values of the ionized electron momentum k for which the transition amplitude are calculated are $k > k'$, a correct numerical calculation of the cross-sections can be achieved using the prior or the complete post versions of the CDW theory. For all other cases, the use of the hybrid theory CDWH is advised.

3. Results and Discussion

In Figure 1, the ionization DDCSs are shown for the case of 1.5 MeV/u F^{9+} and H^+ projectiles over He targets as a function of emission energy for a 0° fixed emission angle. The theoretical cross-sections were calculated using both the prior and complete post versions of the CDW theory using different strategies for the numerical integration: a Gauss quadrature was used using in one case 20 integration points and 60 in the other, as well as a more sophisticated adaptive-step routine from the well-known QUADPACK library [23]. Results show that different results are obtained with each integration strategy. Furthermore, with the increasing level of accuracy in the numerical integration, the difference (overestimation) between the theoretical cross-sections and the experimental results increases. These are both clear indicators that it is not possible to obtain a reliable result from a numerical integration for either version of the CDW theory. Results also show that the calculations arising from the prior and complete post versions give almost the same results when integrated with the same technique. This is in alignment with previous findings regarding post-prior discrepancies in the CDW-EIS theory [11].

Furthermore, in Figure 1, by a discontinuity in the curves, the emission energy ε_f can be identified, corresponding to the k-value for which $K_{min} = K'$: $k = 15.439$ a.u., $\varepsilon_f = 3243$ eV. For values of the k momentum higher than 15.439 a.u. (or ε_f emission energy larger than 3243 eV), there are no more values for the K momentum transfer for which $\alpha+\beta = 0$; therefore, there is no divergence in the integration interval, and all numerical techniques give the same results. According to these findings, the use of either the prior or the complete post versions of the CDW theory for the DDCS calculation is not advised without further checking if the K' value falls inside the integration interval.

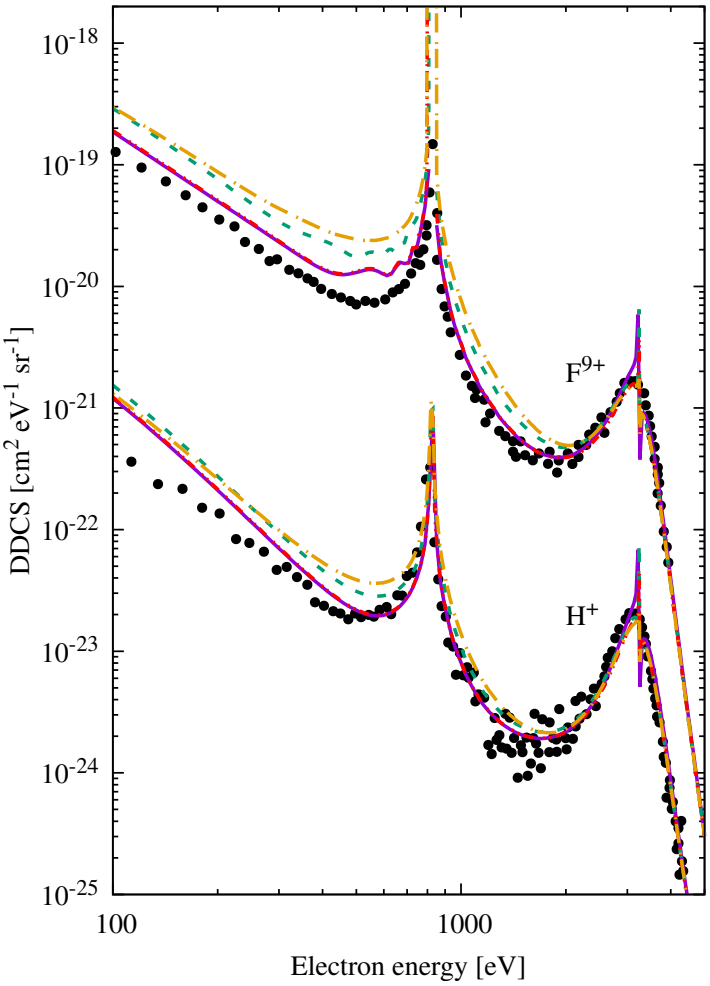

Figure 1. Double differential cross-section for the single ionization of He atoms by 1.5 MeV/u F^{9+} and H^+ impact as a function of the electron energy for a 0° fixed emission angle. Theory: full-line prior CDW integrated with a 20-point Gauss quadrature; dashed-double-dotted-line, complete post CDW integrated with a 20-point Gauss quadrature; dashed-line, complete post CDW integrated with a 60-point Gauss quadrature; dashed-dotted-line, complete post CDW integrated with QUADPACK library; experiments, circles [24].

Figure 2 shows results for the same systems as Figure 1, but in this case, the usual post version and the new complete hybrid post version (as defined in Section 2.3) were used to calculate the corresponding DDCS. Both calculations are in good qualitative agreement with the experiments. As mentioned above in the Theory Section, in the (usual) post version of the CDW, the interaction between the active electron and the target passive ones is included through an effective Coulomb target potential, and in the complete hybrid post version, the residual terms of the target potential are considered, hence taking into account the so-called target dynamic screening having to replace the initial channel projectile distortion by its asymptotic form in order to avoid divergences. Therefore, the contribution of the dynamic screening can be inferred from the difference between the curves corresponding to these two theories. The theoretical results are also compared with the CDW calculations performed by Gulyás and Fainstein [10]. In [10], the numerical target bound-initial and final-continuum states were considered; hence, the dynamic screening is considered exactly in both the initial and exit channel with the drawback that much larger computational times are required.

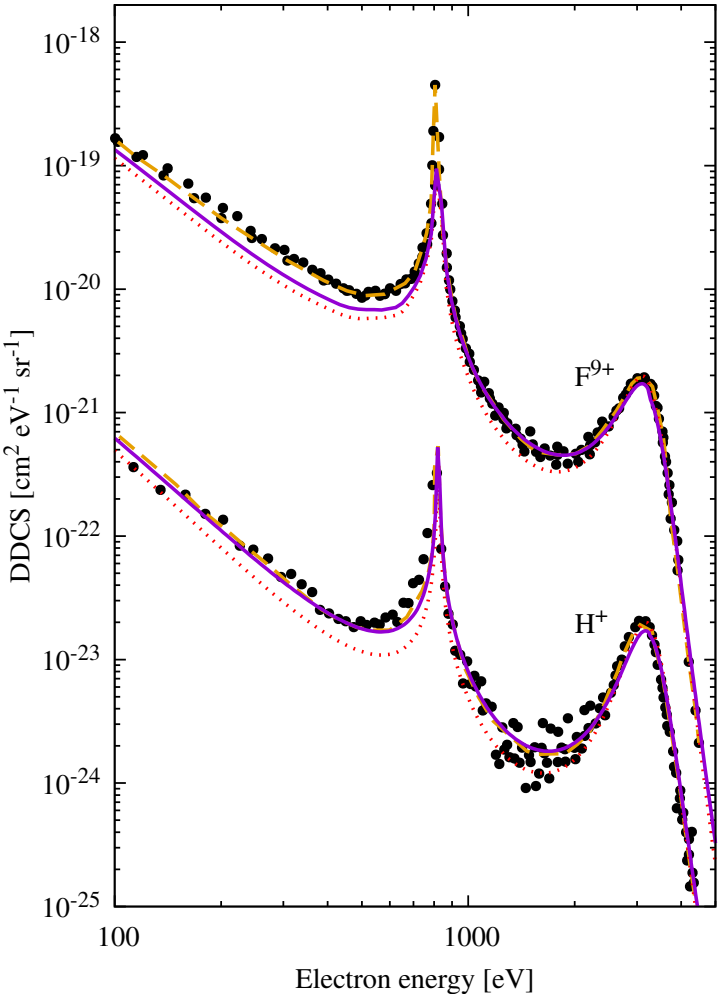

Figure 2. Double differential cross-section for the single ionization of He atoms by 1.5 MeV/u F^{9+} and H^+ impact as a function of the electron energy for a 0° fixed emission angle. Theory: dotted-line, post CDW; full-line, complete hybrid post CDW; dashed-line, CDW theory from [10]; experiments, circles [24].

Figures 3 and 4 show the results for the ionization of He and Ne atoms, respectively, by 6 MeV/u C^{6+} impact as a function of the electron energy for several fixed emission angles. Furthermore, the post and the complete hybrid post versions of the CDW were used to perform the DDCS calculations. It can be clearly seen that the difference between the results obtained with each version are larger, for all angles considered, in the Ne case, which is a consequence of the the dynamic screening being dependent on the residual target electronic distribution.

In Figure 5, together with the ionization DDCS presented in Figures 3 and 4 for a 60° emission angle, the percentage of relative difference (PRD) between post and complete hybrid post calculations is also shown. The PRD is here calculated as $(B - A)/A \times 100$, A (B) being the post (complete hybrid post) calculations. The larger values of PRD are found at a 0° emission angle, and then decrease as the emission angle increases. In the cases presented in Figure 5, it can be seen that the difference between both versions of the CDW theory can be a percentage of 20–60% in the He case and 40–60% in the Ne case. The negative PRD shown in both cases corresponds to the overestimation of the binary peak by the post version of the CDW, which is corrected when considering the dynamic screening. This overestimation of the binary peak by the post version of the CDW-EIS was studied in [11].

Finally, Figure 6 shows the ionization DDCS for Ar targets and 1 MeV H^+ projectiles. These results show that the contribution of the dynamic screening can be considerably large even in the binary-encounter process. As mentioned above, the dynamic screening will not always increase the DDCS, as a previously overestimated binary-encounter peak, in the case of the post version, is corrected when the residual target potential terms are considered.

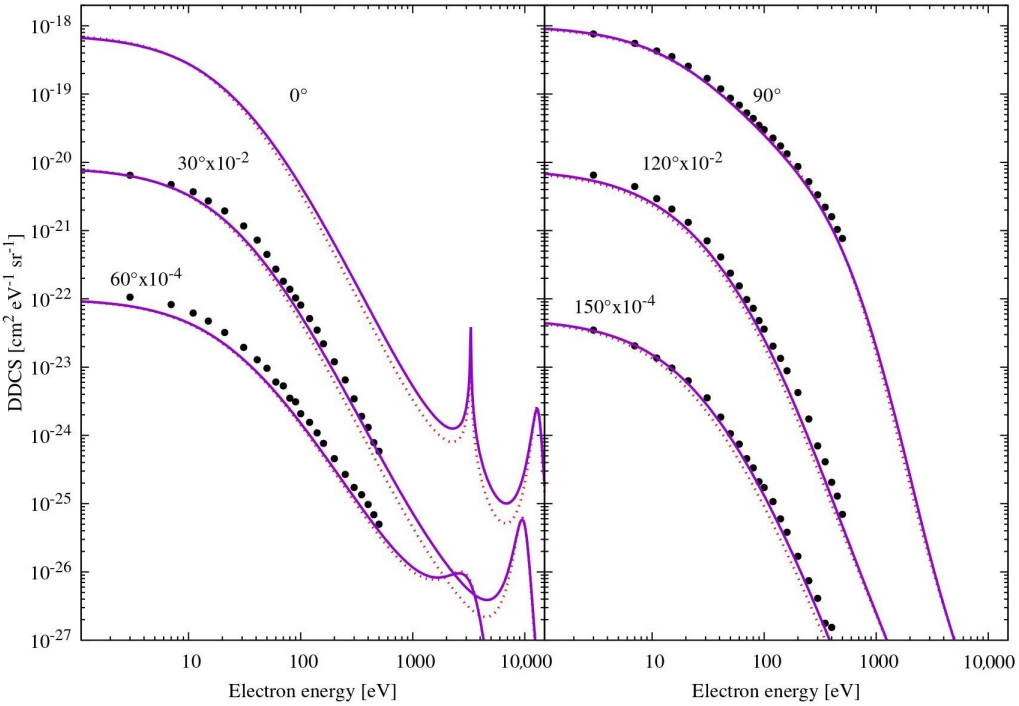

Figure 3. Double differential cross-section for single ionization of He atoms by 6 MeV/u C^{6+} impact as a function of the electron energy for a fixed emission angle. Theory: dotted-line, post CDW; full-line, complete hybrid post CDW; experiments, circles [25].

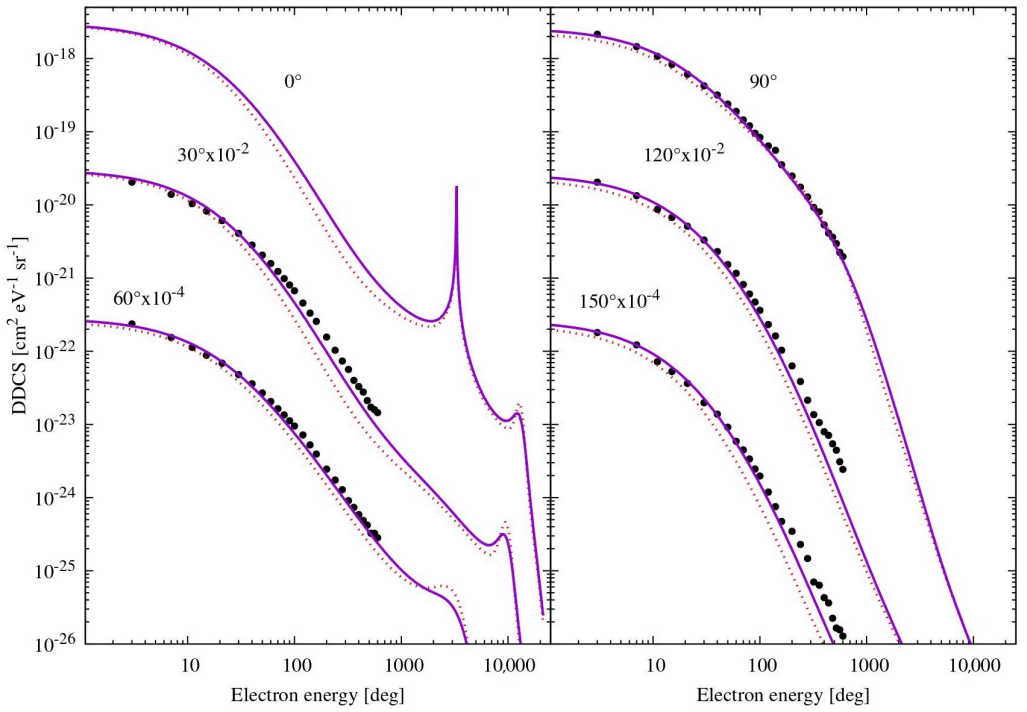

Figure 4. Same as Figure 3, but for the ionization of Ne atoms.

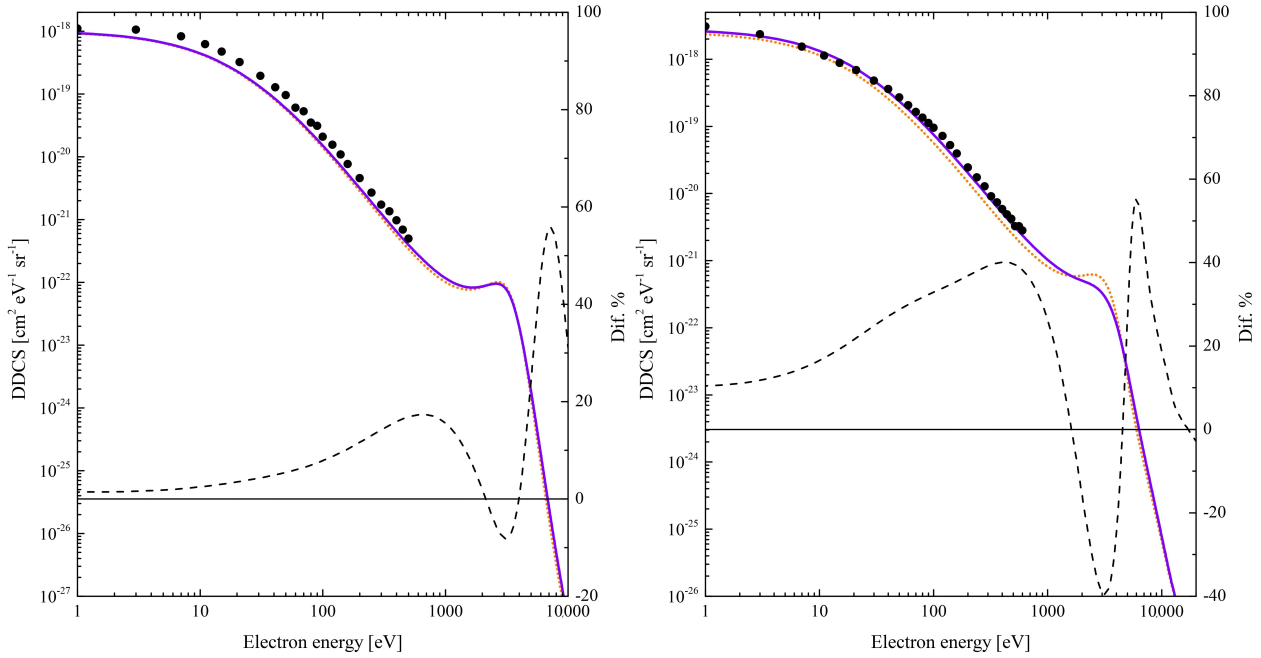

Figure 5. Ionization DDCS of He (left panel) and Ne (right panel) by 6 MeV/u C^{6+} impact for a fixed 60° emission angle as shown in Figures 3 and 4. Dashed lines show the percentage of the relative difference (right axis) between post and complete hybrid post CDW calculations.

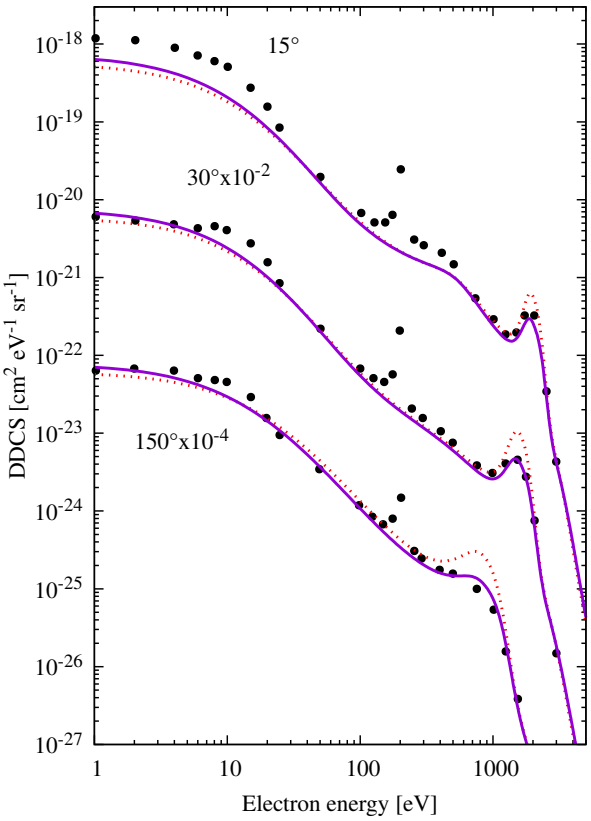

Figure 6. Same as Figure 3, but for the ionization of Ar atoms by 1 MeV H^+ impact. Experiments, circles [26].

4. Conclusions

The CDW theory is revised in order to include the target dynamic screening through the consideration of target-potential residual terms that were previously neglected when working with the post version of the CDW. It is shown that the intrinsic divergences present in the transition amplitude of the prior version of the CDW are avoided when, in the post version, the target potential is approximated by an effective Coulomb one. These divergences reappear in the complete post version when the target-potential residual terms are considered. To this account, we propose to approximate, only in those terms, the initial channel projectile distortion by its asymptotic form: an eikonal phase. This leads to a new theory that takes into account the target dynamic screening without the divergences that prohibit the numerical integration for cross-section calculation. We show results comparing this new theory with the usual post CDW showing the collaboration of the target dynamic screening to the DDCS for He, Ne, and Ar targets.

Furthermore, a detailed study of the intrinsic divergences in the prior and complete post versions of the CDW is performed showing that when the divergence is present on the integration interval, the cross-section calculations strongly depend on the integration technique, whereas for some values of emission energy (depending also on the collision energy and orbital binding energy), the divergence can fall outside the integration interval, and in those cases, a clean numerical integration of the transition amplitude can be achieved to obtain the DDCS. Therefore, the use of either the prior or complete post versions of the CDW to calculate the ionization DDCS is not advised without a previous study of the presence of divergences. This can be troublesome in the case of having to calculate a large set of differential or total cross-sections. In that case, the use of the new complete hybrid post version of the CDW is recommended given that it considers the target dynamic screening and is free of divergences in its transition amplitude.

In a future work, we will investigate the inclusion of the target-potential residual terms when dealing with simple molecular targets.

Author Contributions: Conceptualization, J.M.M. and M.A.Q.; methodology, J.M.M. and M.A.Q.; software, J.M.M. and M.A.Q.; validation, J.M.M. and M.A.Q.; formal analysis, J.M.M. and M.A.Q.; investigation, J.M.M. and M.A.Q.; resources, R.D.R.; data curation, J.M.M., M.A.Q., and R.D.R.; writing, original draft preparation, J.M.M. and M.A.Q.; writing, review and editing, J.M.M., M.A.Q., and R.D.R.; visualization, J.M.M. and M.A.Q.; supervision, R.D.R.; project administration, R.D.R.; funding acquisition, R.D.R. All authors read and agreed to the published version of the manuscript.

Funding: This work received financial support from the Agencia Nacional de Promoción Científica y Tecnológica (ANPCYT) through the project PICT 2015-3392 institution from República Argentina.

Institutional Review Board Statement: Not applicable.

Informed Consent Statement: Not applicable.

Data Availability Statement: All data generated or analysed during this study are included in this published article (and Appendix A).

Conflicts of Interest: The authors declare no conflict of interest.

Abbreviations

The following abbreviations are used in this manuscript:

CDW	Continuum distorted wave
CDW-EIS	Continuum distorted wave-eikonal initial state
GSZ	Green–Sellin–Zachor

Appendix A. Fourier Transforms Depending on ϕ_i and ϕ_f

Each initial target bound state is described as a linear combination:

$$\phi_i = \sum_j C_j \chi_{p_j \lambda_j \alpha_j} \tag{A1}$$

with the $\chi_{p\lambda\alpha}$ functions as Slater-type orbitals, given by:

$$\chi_{p\lambda\pm\alpha}(\mathbf{x}) = R_{p\lambda}(x) Y_\lambda^{\pm\alpha}(\hat{\mathbf{x}}), \tag{A2}$$

where:

$$R_{p\lambda}(x) = \frac{(2Z_{p\lambda})^{p+1/2}}{\sqrt{(2p)!}}\, x^{p-1}\, \exp\left(-Z_{p\lambda} x\right), \tag{A3}$$

and $Y_\lambda^{\pm\alpha}$ is a spherical harmonic ($\alpha \geq 0$).

Following the work in [11], a generating function $\varphi(\mathbf{x})$:

$$\varphi(\mathbf{x}) = \exp\left(-\mathrm{i}\,\boldsymbol{\mu}\cdot\mathbf{x} - \beta\, x\right) \tag{A4}$$

can be used to obtain the different $\chi_{p\lambda\alpha}$ functions in (A1), by the action of a differentiation operator $\hat{D}_{p\lambda\alpha}$, so that:

$$\chi_{p\lambda\alpha}(\mathbf{x}) = \hat{D}_{p\lambda\alpha}\varphi(\mathbf{x})\Big|_{\boldsymbol{\mu}=0\,,\,\beta=Z_{p\lambda}}. \tag{A5}$$

Appendix A.1. Fourier Transform in the Prior Versions of CDW

The prior version of the CDW theory has one Fourier transform depending on the target initial bound state and final continuum one:

$$\boldsymbol{F}^-(\boldsymbol{K}) = \frac{-1}{(2\pi)^{3/2}} \int d\boldsymbol{x}\, \exp\left(-\mathrm{i}\boldsymbol{K}\cdot\boldsymbol{x}\right)\phi_f^*(\boldsymbol{x})\boldsymbol{\nabla}_{\boldsymbol{x}}\,\phi_i(\boldsymbol{x}) \tag{A6}$$

As stated above, this $\boldsymbol{F}^-$ factor is the same as in the prior version of the CDW-EIS theory for ionization.

Writing ϕ_i as in (A1) and ϕ_f as in (8) results in:

$$\boldsymbol{F}^-(\boldsymbol{K}) = \frac{-1}{(2\pi)^{3/2}} \sum_j C_j\, \hat{D}_{p_j\lambda_j\alpha_j} \int d\boldsymbol{x}\, \exp\left(-\mathrm{i}\boldsymbol{K}\cdot\boldsymbol{x}\right)\phi_f^*(\boldsymbol{x})\boldsymbol{\nabla}_{\boldsymbol{x}}\,\varphi(\mathbf{x})\Big|_{\boldsymbol{\mu}=0\,,\,\beta=Z_{p_j\lambda_j}} \tag{A7}$$

$$= \frac{\mathrm{i}}{8\,\pi^{5/2}}\, N(\lambda) \sum_j C_j\, \hat{D}_{p_j\lambda_j\alpha_j} \left[\boldsymbol{\mu}\, J^{(1)} + \beta\, \boldsymbol{J}^{(2)}\right]\Big|_{\boldsymbol{\mu}=0\,,\,\beta=Z_{p_j\lambda_j}} \tag{A8}$$

with:

$$J^{(1)} = \frac{\left(1-G_{\beta\mu}\right)^{-1-\mathrm{i}\lambda}}{\alpha_{\beta\mu}^2}\left[(\mathrm{i}\lambda-1)\,\beta\, G_{\beta\mu} + \beta + \lambda\, k\right] \tag{A9}$$

$$\boldsymbol{J}^{(2)} = \frac{\left(1-G_{\beta\mu}\right)^{-1-\mathrm{i}\lambda}}{\alpha_{\beta\mu}^2}\left[\mathrm{i}\lambda\,\boldsymbol{k} - (1+(\mathrm{i}\lambda-1)\,G_{\beta\mu})(\boldsymbol{K}+\boldsymbol{k}+\boldsymbol{\mu})\right] \tag{A10}$$

and:

$$\alpha_{\beta\mu} = \frac{1}{2}\left[(\boldsymbol{K}+\boldsymbol{k}+\boldsymbol{\mu})^2 + \beta^2\right] \tag{A11}$$

$$G_{\beta\mu} = \frac{[\boldsymbol{k}\cdot(\boldsymbol{K}+\boldsymbol{k}+\boldsymbol{\mu}) + \mathrm{i}\beta\, k]}{\alpha_{\beta\mu}} \tag{A12}$$

Appendix A.2. Fourier Transforms in the Post Versions of CDW

The post version of the CDW theory has two Fourier transforms depending on the target initial bound state and final continuum one, $\boldsymbol{F}^{a+}$ and F^{b+}, given by (27) and (29), respectively. Proceeding in the same way as in Appendix A.1 $\boldsymbol{F}^{a+}$ results in:

$$\boldsymbol{F}^{a+}(\boldsymbol{K}) = \frac{-1}{(2\pi)^{3/2}} \int d\boldsymbol{x} \, \exp\left(-\mathrm{i}\boldsymbol{K}\cdot\boldsymbol{x}\right)\phi_i(\boldsymbol{x})\boldsymbol{\nabla}_{\boldsymbol{x}}\,\phi_f^*(\boldsymbol{x}) \tag{A13}$$

$$= \frac{-\mathrm{i}\lambda}{8\,\pi^{5/2}}\, N(\lambda) \sum_j C_j\, \hat{D}_{p_j\lambda_j\alpha_j} \left[\frac{\left(1 - G_{\beta\mu}\right)^{-1-\mathrm{i}\lambda}}{\alpha_{\beta\mu}^2} \left(\mathrm{i}\beta\,\boldsymbol{k} + k\,(\boldsymbol{K} + \boldsymbol{k} + \boldsymbol{\mu})\right) \right]\Bigg|_{\boldsymbol{\mu}=0\,,\,\beta=Z_{p_j\lambda_j}} \tag{A14}$$

The Fourier transform F^{b+} in (29) depends also on the residual target potential $\tilde{V}_T$. This potential has two terms: a pure Coulomb long-range term and a short-range term:

$$\tilde{V}_T(x) = V_{T_C}(x) + V_{T_{sr}}(x) \tag{A15}$$

$$V_{T_C}(x) = -\frac{(q - \tilde{Z}_T)}{x} \tag{A16}$$

$$V_{T_{sr}}(x) = -\frac{(Z_T - q)}{x}\Omega(x) \tag{A17}$$

with $\Omega(x)$ defined as in (25). The $\Omega(x)$ function in each case is fitted by means of five exponentially decreasing functions (see Table A1):

$$\Omega(x) = \sum_{l=1}^{5} C_l \, \exp\left(-Z_l\, x\right) \tag{A18}$$

Table A1. Coefficients C_l and exponents Z_l for the expansion of the Ω function as described in Equation (A18) for each target considered.

He		**Ne**		**Ar**	
$\mathbf{C}_l$	$\mathbf{Z}_l$	$\mathbf{C}_l$	$\mathbf{Z}_l$	$\mathbf{C}_l$	$\mathbf{Z}_l$
1.77350	2.07594	0.67957	1.80073	−2.88392	2.79017
−2.02508	3.40934	−0.49762	3.35937	2.29974	3.13317
−1.62769	2.31277	1.11389	3.39575	0.22797	0.73040
4.98588	2.68460	0.07557	7.26484	0.14760	9.88781
−2.10744	2.21215	−0.37146	3.17105	1.20838	2.22245

The transition amplitude F^{b+} will also have two terms, which, proceeding in the same way as in Appendix A.1, result in:

$$F^{b+}(\boldsymbol{K}) = F_C^{b+}(\boldsymbol{K}) + F_{sr}^{b+}(\boldsymbol{K}) \tag{A19}$$

$$F_C^{b+}(\boldsymbol{K}) = \frac{1}{(2\pi)^{3/2}} \int d\boldsymbol{x}\, \exp\left(-\mathrm{i}\boldsymbol{K}\cdot\boldsymbol{x}\right) V_{T_C}(\boldsymbol{x}) \phi_i(\boldsymbol{x})\, \phi_f^*(\boldsymbol{x}) \tag{A20}$$

$$= \frac{-(q-\tilde{Z}_T)}{8\,\pi^{5/2}}\, N(\lambda) \sum_j C_j\, \hat{D}_{p_j\lambda_j\alpha_j} \left[\frac{\left(1-G_{\beta\mu}\right)^{-\mathrm{i}\lambda}}{\alpha_{\beta\mu}^2}\right]\Bigg|_{\boldsymbol{\mu}=0\,,\,\beta=Z_{p_j\lambda_j}} \tag{A21}$$

$$F_{sr}^{b+}(\boldsymbol{K}) = \frac{1}{(2\pi)^{3/2}} \int d\boldsymbol{x}\, \exp\left(-\mathrm{i}\boldsymbol{K}\cdot\boldsymbol{x}\right) V_{T_{sr}}(\boldsymbol{x}) \phi_i(\boldsymbol{x})\, \phi_f^*(\boldsymbol{x}) \tag{A22}$$

$$= \frac{-(Z_T-q)}{(2\pi)^{3/2}} \sum_{l=1}^{5} C_l \int d\boldsymbol{x}\, \exp\left(-\mathrm{i}\boldsymbol{K}\cdot\boldsymbol{x} - Z_l\, x\right) \frac{1}{x}\, \phi_i(\boldsymbol{x})\, \phi_f^*(\boldsymbol{x}) \tag{A23}$$

$$= \frac{-(Z_T-q)}{8\,\pi^{5/2}}\, N(\lambda) \sum_{l=1}^{5} C_l \sum_j C_j\, N_{jl}\, \hat{D}_{p_j\lambda_j\alpha_j} \left[\frac{\left(1-G_{\beta\mu}\right)^{-\mathrm{i}\lambda}}{\alpha_{\beta\mu}^2}\right]\Bigg|_{\boldsymbol{\mu}=0\,,\,\beta=Z_{p_j\lambda_j}+Z_l} \tag{A24}$$

with

$$N_{jl} = \left[\frac{Z_{p_j\lambda_j}}{\left(Z_{p_j\lambda_j}+Z_l\right)}\right]^{p_j+1/2} \tag{A25}$$

References

1. Belkić, D. A quantum theory of ionisation in fast collisions between ions and atomic systems. *J. Phys. B At. Mol. Phys.* **1978**, *11*, 3529–3552. [CrossRef]
2. Crothers, D.S.F.; McCann, J.F. Ionisation of atoms by ion impact. *J. Phys. B At. Mol. Phys.* **1983**, *16*, 3229–3242. [CrossRef]
3. Fainstein, P.D.; Ponce, V.H.; Rivarola, R.D. A theoretical model for ionisation in ion-atom collisions. Application for the impact of multicharged projectiles on helium. *J. Phys. B At. Mol. Phys.* **1988**, *21*, 287–299. [CrossRef]
4. Fainstein, P.D.; Ponce, V.H.; Rivarola, R.D. Two-centre effects in ionization by ion impact. *J. Phys. B At. Mol. Phys.* **1991**, *24*, 3091–3119. [CrossRef]
5. Galassi, M.E.; Champion, C.; Weck, P.F.; Rivarola, R.D.; Fojón, O.; Hanssen, J. Quantum-mechanical predictions of DNA and RNA ionization by energetic proton beams. *Phys. Med. Biol.* **2012**, *57*, 2081–2099. [CrossRef]
6. Gulyás, L.; Tóth, I.; Nagy, L. CDW-EIS calculation for ionization and fragmentation of methane impacted by fast protons. *J. Phys. B At. Mol. Phys.* **2013**, *46*, 075201. [CrossRef]
7. Gulyás, L.; Egri, S.; Ghavaminia, H.; Igarashi, A. Single and multiple electron removal and fragmentation in collisions of protons with water molecules. *Phys. Rev. A* **2016**, *93*, 032704. [CrossRef]
8. Mendez, A.M.P.; Montanari, C.C.; Miraglia, J.E. Ionization of biological molecules by multicharged ions using the stoichiometric model. *J. Phys. B At. Mol. Phys.* **2020**, *53*, 055201. [CrossRef]
9. Mendez, A.M.P.; Montanari, C.C.; Miraglia, J.E. Scaling rules for the ionization of biological molecules by highly charged ions. *J. Phys. B At. Mol. Phys.* **2020**, *53*, 175202. [CrossRef]
10. Gulyás, L.; Fainstein, P.D. CDW theory of ionization by ion impact with a Hartree-Fock-Slater description of the target. *J. Phys. B At. Mol. Phys.* **1998**, *31*, 3297–3305. [CrossRef]
11. Monti, J.M.; Fojón, O.A.; Hanssen, J.; Rivarola, R.D. Single electron ionization of multishell atoms: Dynamic screening and post-prior discrepancies in the CDW-EIS model. *J. Phys. B At. Mol. Phys.* **2013**, *46*, 145201. [CrossRef]
12. Ciappina, M.F.; Cravero, W.R.; Garibotti, C.R. Post–prior discrepancies in the continuum distorted wave–eikonal initial state approximation for ion–helium ionization. *J. Phys. At. Mol. Opt. Phys.* **2003**, *36*, 3775–3786. [CrossRef]
13. Ciappina, M.F.; Cravero, W.R. Post–prior discrepancies in CDW–EIS calculations for ion impact ionization fully differential cross-sections. *J. Phys. B At. Mol. Opt. Phys.* **2006**, *39*, 1091–1100. [CrossRef]
14. Monti, J.M.; Fojón, O.A.; Hanssen, J.; Rivarola, R.D. Influence of the dynamic screening on single-electron ionization of multi-electron atoms. *J. Phys. B At. Mol. Phys.* **2010**, *43*, 205203. [CrossRef]
15. Brauner, M.; Macek, J.H. Ion-impact ionization of He targets. *Phys. Rev. A* **1992**, *46*, 2519–2531. [CrossRef] [PubMed]
16. Dubeé, L.J.; Dewangan, D.P. Reinstating an Ionization Theory beyond Reasonable Doubt. In Proceedings of the ICPEAC XIX Conference, Whistler, BC, Canada, 26 July–1 August 1995; p. 62.
17. Cheshire, I.M. Continuum distorted wave approximation; resonant charge transfer by fast protons in atomic hydrogen. *Proc. Phys. Soc.* **1964**, *84*, 89–98. [CrossRef]
18. Belkić, D.; Gayet, R.; Salin, A. Electron capture in high-energy ion-atom collisions. *Phys. Rep.* **1979**, *56*, 279–369. [CrossRef]

19. Stolterfoht, N.; DuBois, R.D.; Rivarola, R.D. *Electron Emission in Heavy Ion-Atom Collisions*; Springer: Berlin, Germany, 1997.
20. Clementi, E.; Roetti, C. Roothaan-Hartree-Fock Atomic Wavefunctions: Basis Functions and Their Coefficients for Ground and Certain Excited States of Neutral and Ionized Atoms, Z <= 54. *At. Data Nucl. Data Tables* **1974**, *14*, 177. [CrossRef]
21. Gravielle, M.S.; Miraglia, J.E. Some Nordsieck integrals of interest in radiation and atomic collision theories. *Comput. Phys. Commun.* **1992**, *69*, 53–58. [CrossRef]
22. Szydlik, P.P.; Green, A.E. Independent-particle-model potentials for ions and neutral atoms with Z <= 18. *Phys. Rev. A* **1974**, *9*, 1885–1894. [CrossRef]
23. Piessens, R.; De Doncker-Kapenga, E.; Überhuber, C.W. *Quadpack: A Subroutine Package for Automatic Integration*; Springer: New York, NY, USA, 1983.
24. Lee, D.H.; Richard, P.; Zouros, T.J.M.; Sanders, J.M.; Shinpaugh, J.L.; Hidmi, H. Binary-encounter electrons observed at 0° in collisions of 1-2-MeV/amu H^+, C^{6+}, N^{7+}, O^{8+}, and F^{9+} ions with H_2 and He targets. *Phys. Rev. A* **1990**, *41*, 4816–4823. [CrossRef] [PubMed]
25. Biswas, S.; Misra, D.; Monti, J.M.; Tachino, C.A.; Rivarola, R.D.; Tribedi, L.C. Energy and angular distribution of electrons in ionization of He and Ne by 6-MeV/u bare carbon ions: Comparison with continuum-distorted wave eikonal-initial-state calculations in prior and post forms. *Phys. Rev. A* **2014**, *90*, 052714. [CrossRef]
26. Rudd, M.E.; Toburen, L.H.; Stolterfoht, N. Differential Cross Sections for Ejection of Electrons from Argon by Protons. *At. Data Nucl. Data Tables* **1979**, *23*, 405. [CrossRef]